PIEZOELECTRIC RL SHUNT DAMPING
OF FLEXIBLE STRUCTURES

Jan Høgsberg, Steen Krenk

Department of Mechanical Engineering, Technical University of Denmark
Nils Koppels Allé, building 403, DK-2800 Kongens Lyngby, Denmark
jhg@mek.dtu.dk, sk@mek.dtu.dk

Keywords: RL shunts, Piezoelectric damping, Structural dynamics, Resonant calibration.

Summary: *Resonant RL shunt circuits represent a robust and effective approach to piezo-electric damping, provided that the individual shunt circuit components are calibrated accurately with respect to the dynamic properties of the corresponding flexible structure. The balanced calibration procedure applied in the present analysis is based on equal damping of the two modes associated with the resonant vibration form of the structure. An important result of the presented calibration procedure is the explicit inclusion of a quasi-static contribution from the non-resonant vibration modes of the structure via a single background flexibility parameter. This leads to explicit calibration expressions for the shunt circuit components and it is demonstrated by a simple numerical example that the procedure with correction for background flexibility leads to both equal damping of the two modes and effective response reduction.*

1. INTRODUCTION

Piezoelectric transducers are used in many different scientific and industrial applications for damping and control of the dynamic response of flexible structures [1]. Piezoelectric transducers are very versatile and may be used as for example actuator/sensor pairs in active control schemes [1], as semi-active devices based on various switching techniques [2], or as passive units in which the piezoelectric transducer is shunted to a suitable electric network [3, 4, 5]. Effective passive vibration damping of flexible structures may be obtained by introducing resonant RL shunt circuits, where an inductance L and a resistance R forms an additional resonance together with the inherent capacitance C of the piezoelectric transducer [3, 4]. This resonance can be synchronized with the structural frequency of the targeted vibration mode and thereby effectively increase the damping level and reduce the vibration amplitudes of the flexible structure, provided that the individual circuit components are calibrated appropriately [6].

The classic calibration procedures for the series RL shunt circuit dates back to Hagood and von Flotow [3], proposing both a frequency response calibration and a pole-placement technique based on a root-locus analysis. The frequency response calibration for the parallel RL shunt was shortly after proposed by Wu [4] and a summary of calibration techniques for both types of RL shunt circuits is provided by Caruso [7]. Alternative calibration procedures have recently been proposed in [8, 9, 10, 11].

The original work by Hagood and von Flotow [3] demonstrates that for RL shunt damping optimal frequency response calibration is in fact non-optimal with respect to a root-locus analysis, while optimal pole placement corresponds to non-optimal dynamic amplification properties. However, for the classic tuned mass absorber the fixed point frequency calibration is equivalent to equal damping in the two modes associated with the targeted vibration form, as demonstrated by Krenk [12]. Furthermore, the device damping is calibrated to provide an optimal combination of response reduction of the structure and limited absorber motion. Exact equivalence between equal modal damping and optimal response reduction appears to be a specific property of the mechanical tuned mass absorber, and is therefore not directly available for the present RL shunt circuit formats. However, as demonstrated in Krenk and Høgsberg [13] for general control formats and in Høgsberg and Krenk [10] for RL shunt circuits the balanced calibration technique with equal modal damping in fact also provides proper reduction of the frequency response amplitudes. Thus, the balanced calibration procedure is here adopted for the calibration of the shunt circuit components.

The performance of a resonant damping concept is very sensitive to even a small detuning of the resonant filter parameters. However, the calibration of resonant damping strategies is typically based on an approximate single mode representation of the flexible structure dynamics, where the interaction with non-resonant vibration modes is neglected. For mechanical vibration absorbers this is often an adequate assumption because mechanical absorbers with an oscillating absorber mass operate with respect to absolute motion [14, 12]. This is different for two-terminal piezoelectric transducers, which act on the deformation of the structure. As demonstrated in the following the efficiency of piezoelectric RL shunt circuit damping depends very much on the precise parameter calibration and thus the influence from the residual non-resonant vibration modes must be included in the calibration expressions for the shunt circuit components. The inclusion of the influence from residual vibration modes by a quasi-static representation has previously been suggested for calibration of resonant active control strategies [15] and tuned mass vibration absorbers [16], and this principle is in the present case applied to piezoelectric RL shunt circuit damping [17].

2. THE ELECTROMECHANICAL SYSTEM

The performance of piezoelectric RL shunt circuit damping relies on a precise balance between the dynamics of the flexible structure and the electric circuit. Thus, the present section presents the electric and mechanical models, which are used for calibration of the shunt circuit parameters in the subsequent section.

2.1 The electric system

As shown in Figure 1(a) the piezoelectric transducer is described by a time variable current source $i_p(t)$ in parallel with a capacitance C, see [18]. The corresponding series and parallel configurations of a resonant RL shunt circuit are shown in Figures 1(b,c). The current flowing into the piezoelectric transducer must be equal to the sum of the current in the current source
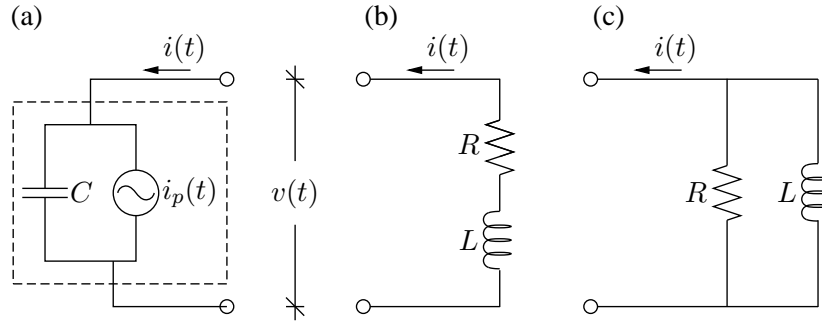
Jan Høgsberg, Steen Krenk

Figure 1. Electric model of (a) piezoelectric transducer, and (b) series or (c) parallel RL shunts.

produced by the deformation of the piezoelectric transducer and the current in the capacitor. When integrating this current relation the following classic charge balance equation is obtained,

$$q(t) = -\theta u(t) + C v(t) \tag{1}$$

where $q(t)$ is the charge in the piezoelectric transducer, $u(t)$ is the deformation of the transducer, while $v(t)$ is the voltage across the transducer terminals. Thus, θ represents the electromechanical coupling coefficient of the piezoelectric transducer.

2.1.1 Series shunt

For the series shunt circuit in Fig. 1b the voltage across the circuit terminals is equal to the sum of the voltage across the resistance R and inductance L, which leads to the following relation between voltage $v(t)$ and charge $q(t)$,

$$v(t) = -\big(R\dot{q}(t) + L\ddot{q}(t)\big) \tag{2}$$

Elimination of charge $q(t)$ between (1) and (2) followed by division with LC gives the normalized filter equation for the piezoelectric transducer with a series RL shunt circuit,

$$\ddot{v}(t) + 2\zeta_e\omega_e\dot{v}(t) + \omega_e^2\, v(t) = \frac{\theta}{C}\big(\ddot{u}(t) + 2\zeta_e\omega_e\, \dot{u}(t)\big) \tag{3}$$

The electric resonance frequency ω_e and damping ratio ζ_e are in this filter equation defined as

$$\omega_e = \frac{1}{\sqrt{LC}} \quad , \quad 2\zeta_e = R\sqrt{\frac{C}{L}} \tag{4}$$

It follows from (3) that the feedback to the filter equation in this case is comprised by a combination of the velocity and acceleration associated with the transducer deformation.

3

2.1.2 Parallel shunt

In Fig. 1c the parallel connection of the resistance R and inductance L implies that the total current in the circuit is equal to the sum of the current in the individual circuit components. This leads to the following relation between voltage and charge,

$$\frac{1}{R}\dot{v}(t) \,+\, \frac{1}{L}v(t) \,=\, -\ddot{q}(t) \tag{5}$$

Elimination of $q(t)$ between (1) and (5) followed by division with C gives the normalized resonant filter equation

$$\ddot{v}(t) \,+\, 2\zeta_e\omega_e\dot{v}(t) \,+\, \omega_e^2\,v(t) \,=\, \frac{\theta}{C}\ddot{u}(t) \tag{6}$$

with frequency and damping parameters

$$\omega_e \,=\, \frac{1}{\sqrt{LC}} \qquad , \qquad 2\zeta_e \,=\, \frac{1}{R}\sqrt{\frac{L}{C}} \tag{7}$$

Compared to the series shunt circuit the present equation in (6) receives pure acceleration feedback, and the filter damping ratio ζ_e is inversely proportional to the circuit resistance R.

2.2 The mechanical system

The dynamics of the flexible structure is represented by a discrete numerical model with the equation of motion

$$\mathbf{M}\ddot{\mathbf{u}}(t) \,+\, \mathbf{K}\mathbf{u}(t) \,=\, \mathbf{w}f(t) \,+\, \mathbf{f}_e(t) \tag{8}$$

In this equation the column vector $\mathbf{u}(t)$ contains the degrees of freedom of the numerical model, the mass matrix $\mathbf{M}$ and stiffness matrix $\mathbf{K}$ represent the inertia and elastic properties of the combined structure, while the column vector $\mathbf{f}_e(t)$ represents the external loading on the structure. The first term on the right hand side of (8) represents the electromechanical force on the structure from the piezoelectric transducer, where the connectivity vector $\mathbf{w}$ defines the deformation of the transducer as

$$u(t) \,=\, \mathbf{w}^T\mathbf{u}(t) \tag{9}$$

In the present case the electromechanical force $f(t)$ is represented in terms of the voltage $v(t)$,

$$f(t) \,=\, -\,\theta v(t) \tag{10}$$

with the electromechanical coupling coefficient θ as scaling factor. It is seen that this electromechanical force term in (8) vanishes for $v(t) \,=\, 0$, and the stiffness matrix $\mathbf{K}$ in (8) therefore represents the elastic stiffness of the structure with the piezoelectric transducer attached with short-circuited electrodes.

The equivalent structural properties are conveniently identified from the frequency representation of (8), which is obtained by introducing the harmonic exponential representations

$\mathbf{u}(t) = \mathbf{u}e^{\mathrm{i}\omega t}$ and $f(t) = fe^{\mathrm{i}\omega t}$ with angular frequency ω and frequency amplitudes $\mathbf{u}$ and f. In the absence of external loading the equation of motion (8) can be written as

$$[\,\mathbf{K} - \omega^2 \mathbf{M}\,]\,\mathbf{u} \;=\; \mathbf{w}f \tag{11}$$

The transducer deformation u is obtained by inverting the above relation,

$$u \;=\; \mathbf{w}^T \mathbf{u} \;=\; \left(\mathbf{w}^T[\,\mathbf{K} - \omega^2\mathbf{M}\,]^{-1}\,\mathbf{w}\right)f \tag{12}$$

The inverse of the system matrix $[\,\mathbf{K} - \omega^2\mathbf{M}\,]$ can be represented in terms of the eigenvectors $\mathbf{u}_1, \cdots, \mathbf{u}_n$ and eigenfrequencies $\omega_1, \cdots, \omega_n$ of the corresponding generalized eigenvalue problem in (11) associated with $f = 0$. Introducing an eigenvector representation of the displacement and force vector in (11) the dynamic flexibility matrix can be written as

$$\left[\,\mathbf{K} - \omega^2\mathbf{M}\,\right]^{-1} \;=\; \sum_{j=1}^{n} \frac{\omega_j^2}{\omega_j^2 - \omega^2} \frac{\mathbf{u}_j \mathbf{u}_j^T}{\mathbf{u}_j^T \mathbf{K} \mathbf{u}_j}\,. \tag{13}$$

The dynamic flexibility at the transducer location in (12) then follows in the form

$$\mathbf{w}^T\left[\,\mathbf{K} - \omega^2\mathbf{M}\,\right]^{-1}\mathbf{w} \;=\; \sum_{j=1}^{n} \frac{\omega_j^2}{\omega_j^2 - \omega^2} \frac{1}{k_j} \;\simeq\; \frac{\omega_r^2}{\omega_r^2 - \omega^2} \frac{1}{k_r} + \sum_{j \neq r}^{n} \frac{1}{k_j} \tag{14}$$

where the modal parameters are associated with the mode shape vector $\mathbf{u}_j/(\mathbf{w}^T\mathbf{u}_j)$ normalized to unity over the transducer. Thus, the modal stiffness, mass and load are defined as

$$k_j \;=\; \frac{\mathbf{u}_j^T \mathbf{K} \mathbf{u}_j}{(\mathbf{w}^T\mathbf{u}_j)^2} \quad , \quad m_j \;=\; \frac{\mathbf{u}_j^T \mathbf{M} \mathbf{u}_j}{(\mathbf{w}^T\mathbf{u}_j)^2} \quad , \quad f_j(t) \;=\; \frac{\mathbf{u}_j^T}{\mathbf{w}^T\mathbf{u}_j}\,\mathbf{f}_e(t) \tag{15}$$

In the latter expression in (14) only the resonant term with $j = r$ is now retained in its frequency-dependent form, while the remaining non-resonant terms are replaced by their equivalent quasi-static solution. The last sum can thus be expressed directly by the expansion in (14) for $\omega = 0$,

$$\mathbf{w}^T \mathbf{K}^{-1} \mathbf{w} \;=\; \sum_{j=1}^{n} \frac{1}{k_j} \;=\; \frac{1}{k_r} + \sum_{j \neq r}^{n} \frac{1}{k_j} \;=\; \frac{1}{k_r} + \frac{1}{k_0} \tag{16}$$

The background flexibility $1/k_0$ is therefore formed by the sum of the quasi-static flexibility of all the non-resonant modes. When introducing (14) into the equation (12) the transducer deformation is obtained in pure scalar form as

$$u \;\simeq\; \left[\,\frac{\omega_r^2}{\omega_r^2 - \omega^2} \frac{1}{k_r} + \frac{1}{k_0}\,\right] f \tag{17}$$

This relation connects the local deformation u of the piezoelectric transducer and the corresponding local piezoelectric force f. In the time domain the expression in (17) represents the

local deformation $u(t)$ as the sum of a resonant modal deformation $u_r(t)$ and an additional quasi-static term $f(t)/k_0$. Thus, the solution in (17) can be written as

$$u(t) \; = \; u_r(t) \; + \; \frac{1}{k_0} f(t) \tag{18}$$

where modal deformation $u_r(t)$ follows from the classic modal equation

$$m_r \ddot{u}_r(t) \; + \; k_r u_r(t) \; = \; f(t) \; + \; f_r(t) \tag{19}$$

associated with the normalized mode shape vector $\mathbf{u}_r/(\mathbf{w}^T \mathbf{u}_r)$. The modal mass m_r and modal load $f_r(t)$ are together with the modal stiffness k_r defined by the general modal relations in (15). In (19) the piezoelectric force $f(t)$ also constitutes the corresponding modal force due to the particular normalization of the resonant mode.

3. EXPLICIT PARAMETER CALIBRATION

The calibration procedure of the present paper is based on the fourth-order characteristic equation in ω obtained by combining the frequency representation of the modal dynamic equation (19) with the corresponding filter equation in (3) for the series circuit or in (6) for the parallel circuit. The influence of background flexibility from the non-resonant vibration modes is taken explicitly into account by the relation in (18). The calibration is based on the principle of equal damping of the two modes associated with the electromechanical system, which is a pole placement principle originally developed for the mechanical tuned mass damper in [12] and recently applied to piezoelectric RL shunt circuit damping in [10, 17]. This section constructs the generic polynomial equation with equal modal damping and presents the calibration procedure based on direct parameter equivalence between the characteristic equations.

3.1 Complex root analysis

Figure 2 shows the desired trajectories of the two complex roots ω_1 and ω_2 with positive real part of the corresponding fourth-order characteristic equation. The two associated vibra-
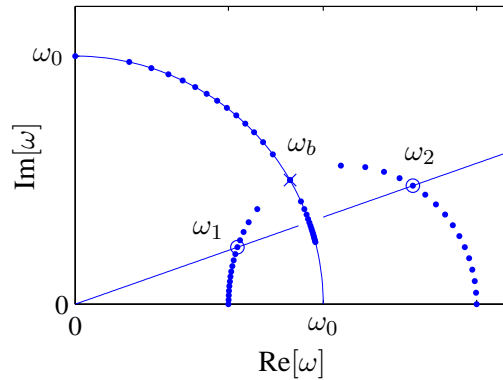

Figure 2. Complex root trajectories with circles indicating solutions ω_1, ω_2.

tion modes will have equal damping ratio if ω_1 and ω_2 lie on the same line containing the origin of the complex plane, as illustrated in the figure. This implies that the roots ω_1 and ω_2 are inverse points with respect to a circle with radius ω_0. This desirable condition can be expressed as $\omega_2/\omega_0 = \omega_0/\omega_1^*$, where the asterisk denotes the complex conjugate. As demonstrated in [12] this reciprocal relation implies a particular form of the fourth-order polynomial equation, which governs the complex-root solution illustrated in Fig. 2. The maximum damping of the individual modes is obtained at the bifurcation point ω_b, where the two complex roots meet. However, at this bifurcation point the two angular frequencies of the modes are identical ($\omega_1 = \omega_2$), which implies constructive interference of the two vibration forms and thereby an undesirable single peak in the dynamic response amplification, as illustrated in [3, 12]. It has been thoroughly demonstrated in [12] that an optimal balance between the attained damping ratio and a suitable separation of the vibration frequencies to avoid interference is obtained by the two roots indicated by the circles in Fig. 2. By construction it can be shown that these complex roots are solutions to the generic equation

$$\omega^4 \,-\, \left(2 + 4\xi^2\right)\omega_0^2\omega^2 \,+\, \omega_0^4 \,-\, 2i\sqrt{2}\xi\omega_0\omega\left(\omega^2 - \omega_0^2\right) \,=\, 0 \tag{20}$$

where ξ is the single remaining system parameter governing the attainable damping level. The special property of equally damped modes is equivalent to imposing a balance between the cubic and linear terms in (20), whereby they cancel at the reference frequency $\pm\omega_0$. This is the basis of the parameter calibration consider in the following subsections.

The parameter values of interest in connection with control and damping of structures correspond to the part in figure 2, where the roots ω_1 and ω_2 are inverse points in the circle. In this part of the solution interval the two complex roots have the form

$$\omega_{1,2} \,=\, |\omega_{1,2}|\left(\sqrt{1 - \zeta^2} + i\zeta\right) \tag{21}$$

where ζ is the common damping ratio of the two vibration modes associated with the targeted resonance of the structure. A simple expression for the modal damping ratio ζ in terms of the system parameter ξ can be obtained by using the fact that the coefficient of the cubic term in (20) is the sum of the four roots [12]. When using the special symmetry properties of the four roots the following approximate expression is obtained for the common damping ratio

$$\zeta \,\simeq\, \tfrac{1}{2}\sqrt{2}\,\xi \tag{22}$$

This approximate expression can be used to determine the system parameter ξ with respect to a desired damping ratio ζ and subsequently choose the piezoelectric transducer and calibrate the shunt circuit components to achieve the desired level of modal damping.

3.2 Calibration of shunt circuit parameters

The calibration procedure is formulated in terms of the modal response $u_r(t)$ described by the modal equation of motion derived from (19),

$$\ddot{u}_r(t) \,+\, \omega_r^2 u_r(t) \,=\, \omega_r^2 \frac{1}{k_r}\left(f(t) + f_r(t)\right) \tag{23}$$

This equation determines the modal displacement $u_r(t)$ and is therefore combined with a local equation for the transducer force $f(t)$ with feedback from the local deformation of the transducer $u(t)$, which is represented by (18) and includes the effect of background flexibility via the term $f(t)/k_0$.

3.2.1 Series shunt circuit

In the case of the series RL shunt circuit the governing equation (3) relates the voltage $v(t)$ and the local deformation of the transducer $u(t)$. When $u(t)$ is expressed in terms of the modal displacement $u_r(t)$ by (18) and the transducer force is introduced by the relation $f(t) = -\theta v(t)$, the following second order differential equation is obtained

$$(1 + \kappa_0)\Big(\ddot{f}(t) + 2\zeta_e\omega_e\dot{f}(t)\Big) + \omega_e^2 f(t) = -k_r \kappa_r\Big(\ddot{u}_r(t) + 2\zeta_e\omega_e\dot{u}_r(t)\Big) \qquad (24)$$

where the electromechanical coupling relative to the modal stiffness and the background stiffness are defined as

$$\kappa_r = \frac{\theta^2}{Ck_r} \qquad , \qquad \kappa_0 = \frac{\theta^2}{Ck_0} \qquad (25)$$

The dynamic equations (23) and (24) are now expressed in the frequency domain, and the natural vibration frequencies ω therefore follow from the associated characteristic equation,

$$\omega^4 - \Big((1 + \kappa_r + \kappa_0)\omega_r^2 + \omega_e^2\Big)\frac{\omega^2}{1 + \kappa_0} + \frac{\omega_e^2\omega_r^2}{1 + \kappa_0} - 2i\zeta_e\omega_e\omega\Big(\omega^2 - \frac{1 + \kappa_r + \kappa_0}{1 + \kappa_0}\omega_r^2\Big) = 0 \qquad (26)$$

The calibration procedure consists in establishing equivalence between this characteristic equation and the generic equation in (20).

The first step is to identify the reference frequency ω_0 both from the ratio between the coefficients to the linear and cubic terms and directly from the constant term. Elimination of ω_0 between these two solutions then gives the filter frequency as

$$\omega_e^2 = \frac{(1 + \kappa_r + \kappa_0)^2}{1 + \kappa_0}\,\omega_r^2 \qquad (27)$$

It is seen from this relation that the shunt circuit frequency ω_e is always larger than the resonant modal frequency ω_r of the structure.

The second step in the calibration procedure determines the damping property of the shunt circuit, represented by the filter damping parameter ζ_e. First ζ_e is determined in terms of the generic parameter ξ by comparing the coefficients of the cubic terms in (20) and (26). However, the parameter ξ also follows by comparing the coefficients of the quadratic terms. Elimination of ξ between these two solutions directly determines the optimal filter damping ratio as

$$\zeta_e^2 = \frac{1}{2}\frac{\kappa_r}{(1 + \kappa_0)(1 + \kappa_r + \kappa_0)} \qquad (28)$$

An estimate of the corresponding modal damping ratio ζ is obtained by substitution of the derived expression for ξ into the approximation (22). This gives the following relation between the damping ratio and the electromechanical coupling coefficient

$$\zeta^2 \simeq \frac{1}{8} \frac{\kappa_r}{1 + \kappa_0} \tag{29}$$

where presence of background flexibility via the parameter κ_0 reduces the damping attained for a given generalized electromechanical coupling coefficient κ_r.

3.2.2 Parallel shunt circuit

For the parallel RL shunt circuit the voltage is governed by (6) and then replaced by the transducer force via the relation $f(t) = -\theta v(t)$. Furthermore, the transducer deformation $u(t)$ is again eliminated by (18) and the resulting filter equation can therefore be written as

$$(1 + \kappa_0)\ddot{f}(t) + 2\zeta_e\omega_e\dot{f}(t) + \omega_e^2 f(t) = -k_r \kappa_r \ddot{u}_r(t) \tag{30}$$

In this case the frequency equations corresponding to (23) and (30) are combined, and the corresponding fourth-order characteristic equation in ω is obtained as

$$\omega^4 - \left((1 + \kappa_r + \kappa_0)\omega_r^2 + \omega_e^2\right)\frac{\omega^2}{1 + \kappa_0} + \frac{\omega_e^2\omega_r^2}{1 + \kappa_0} - \frac{2\mathrm{i}\zeta_e\omega_e}{1 + \kappa_0}\omega\left(\omega^2 - \omega_r^2\right) = 0 \tag{31}$$

This equation is rather similar to (26) for the case of a series RL shunt circuit, the only difference occurring in the last term. Again the ratio between the linear and cubic terms identifies ω_0. And since ω_0 is also determined by the constant term in (21) elimination of ω_0 between these two solutions gives the filter frequency

$$\omega_e^2 = (1 + \kappa_0)\omega_r^2 \tag{32}$$

The damping parameter ζ_e is given in terms of ξ by comparing the coefficients of the cubic term, while ξ also follows from the quadratic terms. Again elimination of ξ between these solutions gives the optimal damping parameter,

$$\zeta_e^2 = \tfrac{1}{2}\kappa_r \tag{33}$$

Finally, the attainable modal damping ratio can be estimated by the approximation in (22), where ξ has been determined in connection with the derivation of ζ_e in (33). It turns out that the modal damping ratio ζ in the present case is identical to the expression (29) obtained for the series shunt circuit.

3.3 Design procedure

The design expressions in the previous subsection are given in a format where the generalized electromechanical coupling coefficient θ^2/C is assumed known and the shunt circuit components are then determined. However, the common solution for the estimate of the attainable

Table 1. Calibration of RL shunt circuit components.

	$LC\omega_r^2$	$RC\omega_r$
Series:	$\dfrac{1 + \kappa_0}{(1 + \kappa_0 + \kappa_r)^2}$	$\sqrt{\dfrac{2\kappa_r}{(1 + \kappa_0 + \kappa_r)^3}}$
Parallel:	$\dfrac{1}{1 + \kappa_0}$	$\sqrt{\dfrac{1}{2\kappa_r(1 + \kappa_0)}}$

modal damping ratio in (29) suggests that the electromechanical properties of the piezoelectric transducer may initially be chosen based on a desired level of the modal damping ζ_{des}. Thus, the procedure is conveniently reversed so that it initially obtains an optimal value of θ^2/C based on the desired modal damping ratio ζ_{des}, and then determines the inductance L and resistance R based on the properties of the chosen piezoelectric transducer. Therefore, the desired modal damping ratio ζ_{des} is conveniently assumed given, while the background flexibility coefficient κ_0 is expressed in terms of the modal flexibility coefficient κ_r as $\kappa_0 = (k_r/k_0)\kappa_r$. Hereby, the expression for the modal damping ratio in (29) can be inverted to give the design formula

$$\kappa_r = \frac{8\zeta_{\mathrm{des}}^2}{1 - 8(k_r/k_0)\zeta_{\mathrm{des}}^2} \tag{34}$$

and the actual electromechanical coupling parameter then follows from (25a) as

$$\frac{\theta^2}{C} = \kappa_r\, k_r \tag{35}$$

It is worth noting that the introduction of the background flexibility parameter κ_0 actually leads to a larger design value of the electromechanical coupling coefficient. The shunt circuit components L and R can finally be determined via the respective expressions for the optimal filter parameters ω_e and ζ_e. The explicit design expressions for the shunt circuit components are summarized in Table 1 for both the series and parallel RL shunt circuits.

4. DAMPING OF FLEXIBLE STRUCTURE

The purpose of this final example is both to illustrate the efficiency of the balanced calibration procedure with equal modal damping properties and in particular to demonstrate the importance of including the effect from non-resonant vibration modes via the background flexibility parameter κ_0.

4.1 Beam with piezoelectric transducer

Figure 3 shows two identical piezoelectric transducers placed symmetrically on a cantilever beam. The two piezoelectric transducers are conveniently treated as a single transducer couple

with effective piezoelectric and shunt circuit parameters. The beam is discretized by 10 finite beam elements and the pair of piezoelectric transducers is assumed to exactly occupy the fourth element. The total contribution to the bending stiffness from the transducer couple with short-circuit electrodes is $EI_p = \frac{1}{2}EI$, where EI is the beam bending stiffness. The stiffness matrix is therefore given as

$$\mathbf{K} = \mathbf{K}_b + EI_p\mathbf{w}\mathbf{w}^T \qquad (36)$$

where $\mathbf{K}_b$ is the stiffness matrix of the beam without piezoelectric transducers, while the connectivity vector $\mathbf{w}$ defines the change in rotation $\Delta\varphi_4 = \varphi_4 - \varphi_3 = \mathbf{w}^T\mathbf{u}$ across the transducer element. Finally, the mass of the transducer couple in not included in the mass matrix $\mathbf{M}$.

The piezoelectric transducers are connected to individual resonant shunt circuits with identical resistance R and inductance L. As demonstrated in (34) and (35) the dimensions and properties of the piezoelectric transducer are conveniently chosen or estimated so that a desired value of the modal damping ratio $\zeta = \zeta_{\mathrm{des}}$ is obtained for the resonant vibration mode of the structure. The results from the calibration procedure are presented in Table 2 for the series shunt circuit and in Table 3 for the parallel shunt circuit. For both shunt circuit configurations the calibration is conducted the desired damping ratios $\zeta_{\mathrm{des}} = 0.02$ and 0.04. These results are summarized in the top half of each table, while the bottom half presents the corresponding results for $\kappa_0 = 0$ without correction for background flexibility.

4.2 Root locus analysis

The last column in each of the Tables 2 and 3 gives the damping ratios for the two modes associated with the first vibration form of the beam structure. The damping ratio is determined as $\zeta = \mathrm{Im}[\omega]/|\omega|$, where the complex-valued natural frequency ω is governed by the eigenvalue problem constituted by the homogeneous form of the structural equation of motion (8) together with the filter equation in (3) and (6) for the series and parallel shunt circuits, respectively. The results for the damping ratio in the top half of both tables show that the two damping ratios are virtually identical and equal to the corresponding desired value ζ_{des}. This demonstrates that equal modal damping is obtained when using the present balanced calibration procedure with correction by the non-vanishing background flexibility factor κ_0. In the bottom half of the tables without correction for background ($\kappa_0 = 0$) the equal modal damping property is not retained.
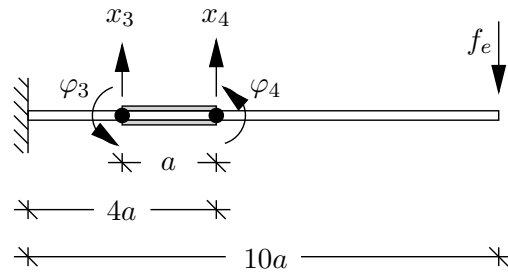

Figure 3. Beam with nodal displacement x_j and rotation φ_j and piezoelectric transducer pair.

Table 2. Complex root analysis: Series RL shunt circuit.

ζ_{des}	κ_r	κ_0	$LC\omega_r^2$	$RC\omega_r$	$\dfrac{\omega_e}{\omega_r}$	ζ_e	ζ
0.02	0.0033	0.0403	0.9551	0.0765	1.0232	0.0392	0.0200 0.0200
0.04	0.0151	0.1834	0.8238	0.1326	1.1018	0.0731	0.0400 0.0399
0.02	0.0032	0.0000	0.9936	0.0796	1.0032	0.0399	0.0290 0.0118
0.04	0.0128	0.0000	0.9749	0.1570	1.0128	0.0795	0.0715 0.0143

In fact, the damping ratio from the first eigenvalue becomes too large, while the damping ratio from the second eigenvalue is reduced, which consequently reduces the effective damping of the resonant structure.

4.3 Frequency response analysis

Figure 4 shows the frequency amplitude of the transverse tip motion u_{tip} of the cantilever beam in (a,b) and the amplitude of the piezoelectric force $f = -\theta v$ in (c,d). The results are obtained from the frequency representation of the equation of motion (8) with the transverse tip force introduced by the load vector $\mathbf{f}_e = [\,0\,\ldots\,,\,f_e\,,0\,]^T$ and the corresponding filter equation (3) or (6). Because the dynamic tip motion amplitude is normalized by the corresponding static deflection u_{tip}^0 the curves in Fig. 4(a,b) represent the so-called dynamic amplification, while the force in Fig. 4(c,d) is normalized by the modal load f_r defined in (15c). Each of the sub-figures in Fig. 4 contain curves for the desired modal damping ratios $\zeta_{\text{des}} = 0.02$ and 0.04, as

Table 3. Complex root analysis: Parallel RL shunt circuit.

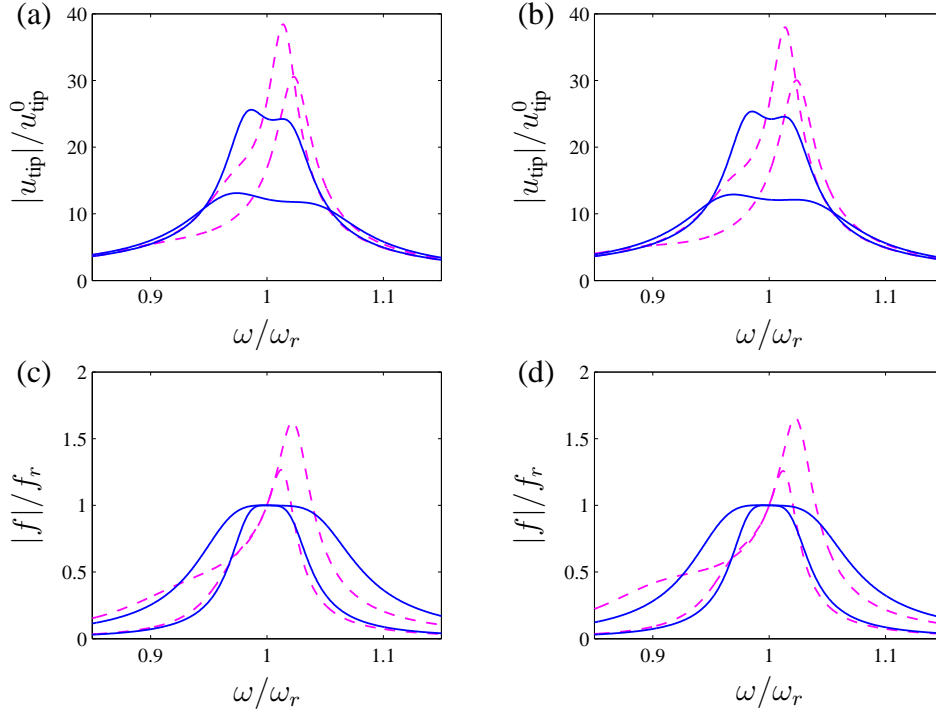| ζ_{des}	κ_r	κ_0	$LC\omega_r^2$	$1/(RC\omega_r)$	$\dfrac{\omega_e}{\omega_r}$	ζ_e	ζ
0.02	0.0033	0.0403	0.9613	0.0832	1.0200	0.0408	0.0200 0.0200
0.04	0.0151	0.1834	0.8450	0.1893	1.0878	0.0870	0.0400 0.0399
0.02	0.0032	0.0000	1.0000	0.0800	1.0000	0.0400	0.0276 0.0117
0.04	0.0128	0.0000	1.0000	0.1600	1.0000	0.0800	0.0601 0.0142

Figure 4. (a,b) Dynamic amplification and (c,d) force amplitude for (a,c) series and (b,d) parallel RL shunt circuit.

also considered in Table 2. The solid curves represent the case with correction for background flexibility, while the dashed curves represent the corresponding case with $\kappa_0 = 0$. It is observed that the solid curves in Fig. 4 show both the desired reduction in the vibration amplitude of the structure and the entirely flat plateau in the magnitude of the piezoelectric force. For both the series (a,c) and the parallel (b,d) shunt circuits the dashed curves exhibit a significant detuning because of the absence of the correction for background flexibility ($\kappa_0 = 0$). For the double peak plateau of the dynamic amplification in Fig. 4(a,b) the left peak is lowered, while the right peak has become larger. This corresponds well with the observed loss of equal modal damping discussed in the previous subsection and illustrated by the results in the bottom rows ($\kappa_0 = 0$) of Table 2. For the present transducer location it is found that the increase in vibration amplitude is approximately 50% compared to the calibration case where the κ_0 correction has been included.

5. CONCLUSIONS

The design of piezoelectric RL shunt circuits is commonly based on a single mode representation of the structural response, whereby the electromechanical system is governed by two coupled scalar equations: The modal equation of motion and the corresponding electric filter equation. Although the electromechanical properties of the piezoelectric transducer have been be determined accurately, the assumed single mode representation is an approximation,

which may result in significant detuning of the actual system. In the present paper the transducer deformation is approximated by the resonant part from the targeted vibration mode and a quasi-static contribution from the remaining non-resonant vibration modes. This representation introduces an additional background flexibility parameter κ_0, which modifies the coefficients of the electric filter equation. As demonstrated the presence of the background flexibility parameter is easily taken into account by the proposed balanced calibration procedure because it is based on full equivalence between the characteristic equations and the desired generic equation with implied equal modal damping. The presented balanced calibration procedure with explicit correction for background flexibility comprises equal modal damping, effective reduction of the dynamic amplification, no peak in the frequency dependent force amplitude, and explicit design expressions for the system parameters. The accuracy of this calibration procedure is illustrated by a numerical example, which initial shows that the presence of the background flexibility parameter leads to a reduction in both inductance and resistance, compared to the calibration expressions with $\kappa_0 = 0$. Furthermore, it is seen that the property of equal modal damping requires this correction for background flexibility, and in the case without correction ($\kappa_0 = 0$) the desired flat plateau of the double peaks in the dynamic amplification is lost.

References

[1] A. Preumont, *Vibration Control of Active Structures. An Introduction*, 3rd edition, Springer, Heidelberg, 2011.

[2] J. Ducarne, O. Thomas, J.-F. Deü, Structural vibration redduction by switch shunting of piezoelectric elements: Modeling and optimization, *Journal of Intelligent Material Systems and Structures* 21 (2010) 797-816.

[3] N.W. Hagood, A. von Flotow, Damping of structural vibrations with piezoelectric materials and passive electrical networks, *Journal of Sound and Vibration* 146 (1991) 243-268.

[4] S.Y. Wu, Piezoelectric shunts with a parallel R-L circuit for structural damping and vibration control, *SPIE Proceedings* 2720 (1996) 259-269.

[5] A. Preumont, B. de Marneffe, A. Deraemaeker, F. Bossens, The damping of a truss structure with a piezoelectric transducer, *Computers and Structures* 86 (2008) 227-239.

[6] O. Thomas, J. Ducarne, J.-F., Deü, Performance of piezoelectric shunts for vibration reduction, *Smart Materials and Structures*, 80 (2012) 235-268.

[7] G. Caruso, A critical analysis of electric shunt circuits employed in piezoelectric passive vibration damping, *Smart Materials and Structures* 10 (2001) 1059-1068.

[8] K. Yamada, H. Matsuhisa, H. Utsuno, K. Sawada, Optimum tuning of series and parallel LR circuits for passive vibration suppression using piezoelectric elements, *Journal of Sound and Vibration* 329 (2010) 5036-5057.

[9] M.V. Kozlowski, D.G. Cole, R.L. Clark, A comprehensive study of the RL series resonant shunted piezoelectric: A feedback controls perspective, *Journal of Vibration and Acoustics* 133 (2011) 011012 (10pp).

[10] J. Høgsberg, S. Krenk, Balanced calibration of resonant shunt cicuits for piezoelectric vibration control, *Journal of Intelligent Material Systems and Structures* 23 (2012) 1937-1948.

[11] Soltani P, Kerschen G, Tondreau and Deraemaeker A (2014) Piezoelectric vibration damping using resonant shunt circuits: an exact solution. *Smart Materials and Structures* 23: 125014 (11pp).

[12] S. Krenk, Frequency analysis of the tuned mass damper, *Journal of Applied Mechanics* 72 (2005) 936-942.

[13] S. Krenk, J. Høgsberg, Equal modal damping design for a family of resonant vibration control formats, *Journal of Vibration and Control* 19 (2013) 1294-1315.

[14] J.P. Den Hartog, *Mechanical Vibrations*, 4th edition, McGraw-Hill, New York, 1956.

[15] S. Krenk, J. Høgsberg, Optimal resonant control of flexible structures, *Journal of Sound and Vibration* 323 (2009) 530-554.

[16] S. Krenk, J. Høgsberg, Tuned mass absorber on a flexible structure, *Journal of Sound and Vibration* 333 (2014) 1577-1595.

[17] J. Høgsberg, S. Krenk, Balanced calibration of resonant piezoelectric RL shunts with quasi-static background flexibility correction, *Journal of Sound and Vibration* 341 (2015) 16-30.

[18] H.H. Law, P.L. Rossiter, G.P. Simon, L.L. Koss, Characterization of mechanical vibration damping by piezoelectric materials, *Journal of Sound and Vibration* 197 (1996) 489-513